LARGE-SCALE ADDITIVE MANUFACTURING OF HIGHLY EXOTHERMIC REACTIVE POLYMER SYSTEMS

Stian K. Romberg[1,2], Christopher J. Hershey[2], John M. Lindahl[2], William Carter[2], Brett G. Compton[1], and Vlastimil Kunc[2]

[1]University of Tennessee, Knoxville
Knoxville, TN

[2]Manufacturing Demonstration Facility
Oak Ridge National Laboratory
Oak Ridge, TN

ABSTRACT

Additive manufacturing (AM) of reactive polymer systems involves the deposition of materials at room temperature that either cure during printing through a chemically initiated reaction or require thermal initiation after printing. This presentation focuses on large-scale AM of chemically initiated thermosetting resins to characterize the effects of heat generation, temperature-dependent viscoelasticity, and crosslinking on the printing process. Real-time tracking of both temperature and cure fronts during the build process were investigated using infrared (IR) and optical vision systems in combination with selected material dyes. Heat generation within the previously-deposited layers was observed to cause significant reduction in the storage modulus (G') and viscosity of newly-deposited layers, resulting in bead instabilities and failure of the print. Quantitative experimental observations on thin-wall structures suggest strategies for mitigating this failure mode through selection of print parameters and tailoring of viscoelastic properties of the feedstock resin.

1. INTRODUCTION

Additive manufacturing (AM) is a process which offers significantly reduced cost and lead time over traditional manufacturing, particularly in production of proof-of-concept test articles [1]. Small-scale polymer AM methods include fused filament fabrication (FFF) using a thermoplastic filament, polyjet and stereolithography (SLA) which photopolymerize a UV curable resin, selective laser sintering (SLS), and reactive deposition involving the mixture of chemically reactive species to form a thermoset part. Both thermoplastic feedstock and thermosetting resins can offer competitive advantages over metals due to their low-cost, low-weight, and rapid manufacturing potential. By utilizing polymer composite technology, AM parts can be tailored to

SAMPE Conference Proceedings. Charlotte, NC, May 20-23, 2019. Society for the Advancement of Material and Process Engineering

have higher strength, improved thermal and electrical conductivity, and higher service temperature compared to unfilled polymer materials.

Large-scale additive manufacturing has revolutionized the AM market by enabling rapid, economical production of molds and tooling [1-2]. The Big Area Additive Manufacturing (BAAM) system is capable of rapid deposition (up to 45 kg/hour) on a large platform (6 m long x 2.5 m wide x 1.8 m tall) using a low-cost pellet feedstock (<$10/kg) [3]. The large-scale BAAM systems have had remarkable success manufacturing high-strength and high-temperature resistant parts out of thermoplastic feedstock with and without filler reinforcement [1-4].

However, thermoplastic AM suffers from several processing and material challenges, including residual stress due to thermal gradients [5] and poor layer-to-layer adhesion [4]. Unlike thermoplastic feedstocks, many thermoset resins have low entanglement densities which allow for room temperature deposition [6-8]. Room temperature deposition reduces thermal gradients, and successive deposition of unreacted liquid layers leads to superior z-axis mechanical properties over thermoplastics after crosslinking [5, 9, 10].

The present study investigates the evolution of thermal gradients in a thin-walled structure printed using an exothermic thermosetting resin on a large-scale AM platform [11]. Depending on the thermoset chemistry, solidification of the printed part due to curing can occur during printing on the deposition bed or after printing in an oven. Both methods, in general, result in significant heating of the part while the resin is still a viscoelastic liquid, resulting in a significant decrease in modulus and part stability. Researchers with an understanding of the new developments within polymer AM are the intended audience of this study.

2. EXPERIMENTATION

2.1 Material

In this study we use exothermic thermosetting resins. The specific chemistry is proprietary, but in general, the results of this work will apply to any chemistry.

Rheological characterization was performed on a TA Instruments DHR-2 rheometer using a parallel plate setup. Adiabatic temperature sweep tests were conducted using a J-type thermocouple inserted into a 500 mL insulated cup. Resin was extruded directly from the AM printhead into the adiabatic cup over four minutes.

2.2 Non-dimensionalization

All absolute values of temperature and time have been non-dimensionalized to protect the intellectual property of our research partners. The temperature scale is normalized by the critical temperature, T_c, which corresponds to the temperature at which the unreacted material attains a minimum storage modulus value. The time scale is normalized by the adiabatic gel time, t_{gel}, the time at which the viscosity doubles after the cross-linking reaction begins under adiabatic conditions.

2.3 Printing

2.3.1 Hardware

Printing was conducted on a large-scale reactive thermoset extrusion printer (2.44 m wide x 4.88 m long x 1.00 m tall) developed by Magnum Venus Products. The deposition nozzle was 5.08 mm (0.200 in) in diameter. The gantry, where the mixing head is attached, has a maximum translation speed of 1270 mm/s (50 in/s). The system is fed by resin and initiator pumps located remotely. The resin and initiator are transferred through the feed lines to mix in the mixing head. After the mixing head, the reacting material is extruded through the nozzle onto the substrate or previous layers, as seen in Figure 1a.

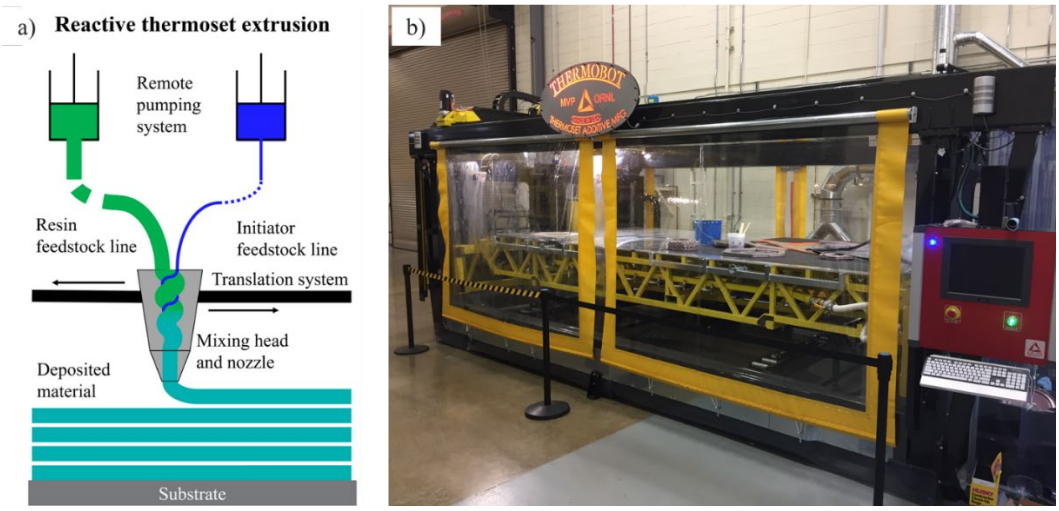

Figure 1. a) Reactive thermoset extrusion schematic b) MVP printer at ORNL

2.3.2

2.3.3 Geometry

A semi-infinite, thin-wall specimen with a normalized layer time of 0.563 (LT_{563}) was printed to shape as outlined in Figure 2. Supporting nodes were added on each end of the thin wall to provide additional resistance to buckling. Temperature varied less than 5% along the bead direction within the viewing window of the IR camera satisfying the semi-infinite assumption.

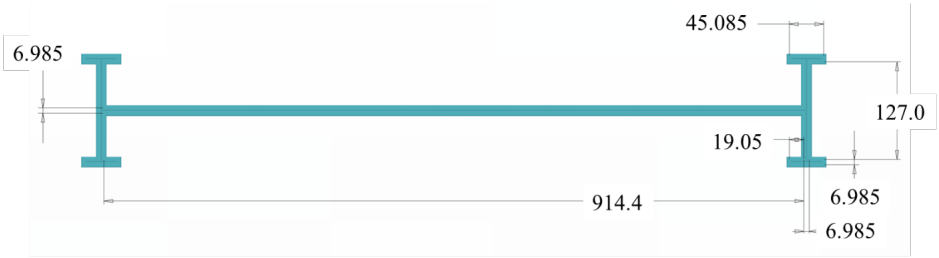

Figure 2. Semi-infinite, thin-wall specimen schematic with dimensions (mm).

2.3.4 Printing parameters

The feed rate in the x- and y-direction was 68.58 mm/s (2.7067 in/s) with a z-direction speed of 13.00 mm/s (0.5118 in/s) and a pump spindle rate of 700 RPM. The resulting layer height and bead spacing were 2.794 mm (0.110 in) and 6.985 mm (0.275 in), respectively.

2.4 Imaging

2.4.1 IR camera

The printing process was recorded using a FLIR A65 IR temperature sensor positioned to observe the broad-side of the wall as can be seen in Figure 3. To obtain desired resolution, the sensor was placed ~279 mm (~11 in) from wall to allow for a viewing window of ~292 mm (~11.5 in) by ~152 mm (~6 in) above the bed. The sensor was programmed to acquire IR data once every second.

2.4.2 Optical camera

A Basler acA4112-8gc optical camera was placed next to the IR camera to monitor the bead geometry of each layer (Figure 3). The data acquisition rate for LT_{563} was 12 images per layer.

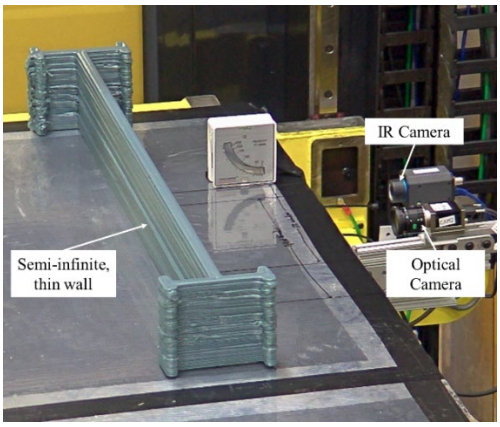

Figure 3. IR and optical camera setup

2.5 IR data analysis

The approximate emissivity of the thermoset resin was determined to be 0.84. Ambient temperature during printing was approximately 18 °C. Point temperature data was extracted from the IR video by placing static "cursors" to obtain data at the cursor locations throughout the entire print, as shown in Figure 4. Cursor data was exported to MATLAB and smoothed using a three-point moving average.

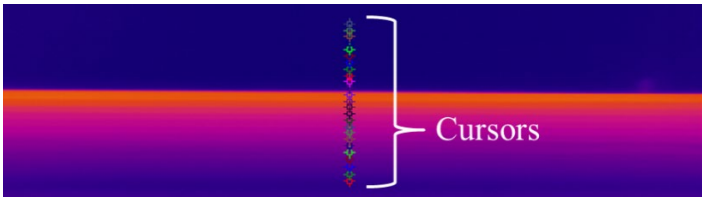

Figure 4. IR cursor locations

3. RESULTS

3.1 Material

The critical temperature, where storage modulus and viscosity decrease to a constant minimum value, was determined by performing a temperature sweep on the uninitiated material, shown in Figure 5a. For the purposes of rationalizing our experimental observations described below, we approximate the curing process as a step function, where the storage modulus of the resin increases instantaneously at the gel time, as illustrated in Figure 5b. Figure 5c shows the adiabatic exotherm from the cross-linking reaction in the thermosetting resin.

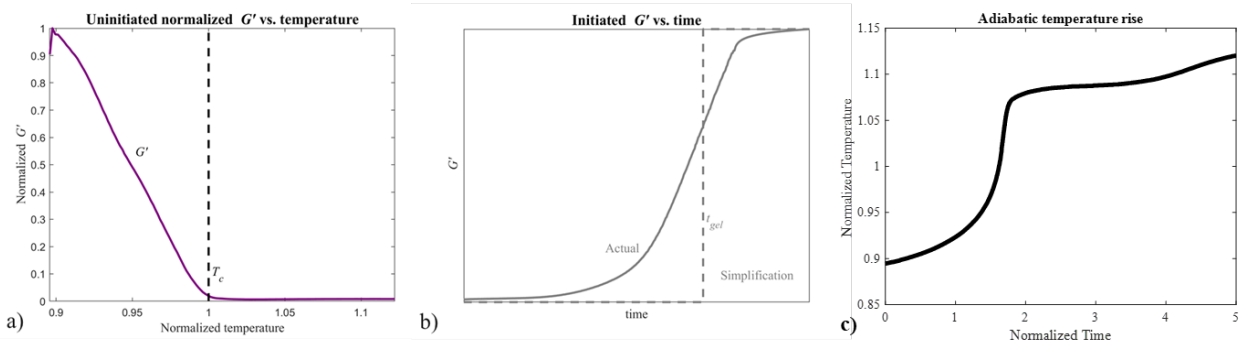

Figure 5. a) Storage modulus of Polynt thermosetting resin as a function of temperature b) Conceptual plot of "actual" and "simplified" behavior of G' with time c) Adiabatic temperature rise data from experiment showing exothermic behavior.

3.2 IR temperature and thermal images

The data output from the IR camera for LT_{563} was organized into temperature vs. time for specified layers (Figure 6a) and temperature vs. height plots for layer time intervals (Figure 6b). Thermal snapshots at critical points in the print are shown in Figure 6c. The thermal history in Figure 6a shows the material successfully passing through an initial temperature spike and reaching a steady-state. Once thermal steady-state is attained, the entire print is able to continue indefinitely.

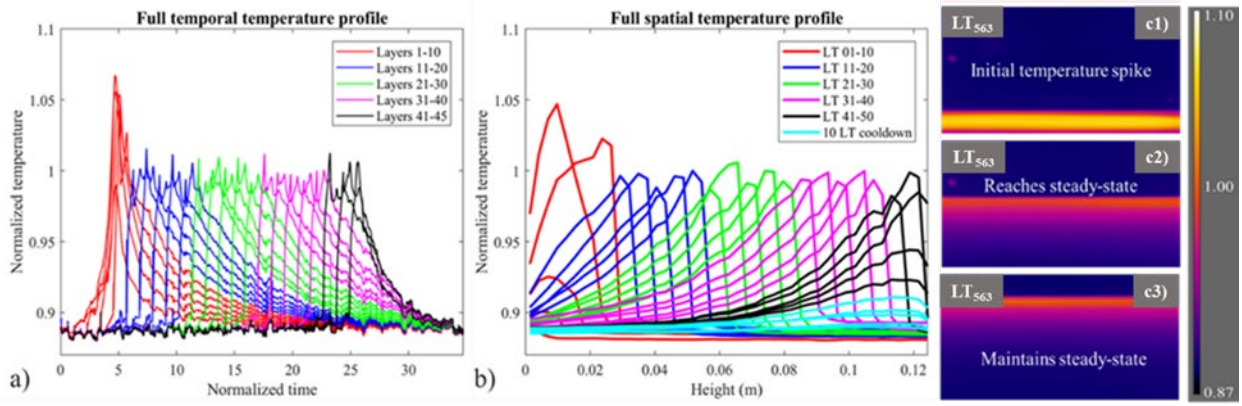

Figure 6. a) Normalized temperature vs. time for LT_{563} (every other layer). b) Normalized temperature vs. height for LT_{563} (every two layer intervals). c) IR thermal evolution for LT_{563}.

3.3 Yield Criterion and Optical Analysis

From the thermal history data, the maximum temperature, and the time to reach maximum temperature was extracted for each printed layer. Comparing these values to constant values of T_c and t_{gel} led to an analysis for interpreting yielding failure. Layers that attained temperatures above T_c at times less than t_{gel} were found to experience yield behavior, thus defining a criterion for yielding-type failure.

LT_{563} exhibited an initial temperature spike, then began to oscillate around a steady-state maximum layer temperature (~layers 15-20). Following the temperature spike, several successive layers (8-11) reached the yielding criteria (Figure 7c) and exhibited yielding (Figure 7a). These yielded layers did not result in failure of the print since subsequent deposition was able to compensate for the loss in height of the yielded layers (Figure 7a).

Inspection of Figure 7c shows that after steady-state was reached, LT_{563} periodically met the yielding criteria, though showed a lower degree of yielding as compared to layers 8-11. This behavior may be attributable to the small temperature differential between the maximum layer temperature and T_c.

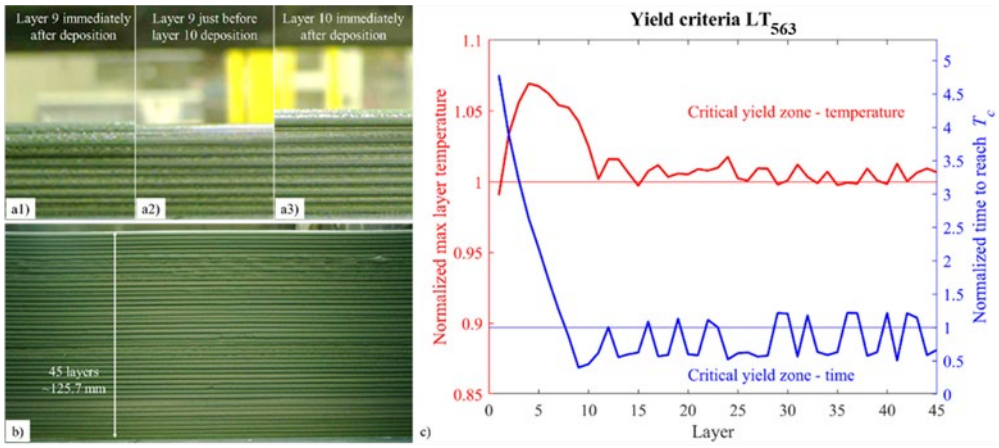

Figure 7. a) Yielding behavior of layer 9 due to the initial temperature spike, followed by deposition of layer 10. b) Full successfully printed wall. c) Normalized max temperature and time to T_c vs. layer to identify yield criteria.

4. SUMMARY

This work demonstrated the successful large-scale additive manufacturing of exothermic reactive polymer systems. The experiment identified a layer time that successfully prints the semi-infinite, thin-wall structure with the thermoset material system. This work also introduced a method to probe the material rheology to identify a critical temperature and adiabatic gel time in order to define a set of yielding criteria to predict when prints are expected to fail.

The next stage of this work will include the development of a thermomechanical model that can guide the selection of print parameters based on the reaction kinetics and viscoelastic properties of the feedstock material to avoid print failure.

5. ACKNOWLEDGEMENTS

Research sponsored by the U.S. Department of Energy, Office of Energy Efficiency and Renewable Energy, Industrial Technologies Program, under contract DE-AC05-00OR22725 with UT-Battelle, LLC.

6. REFERENCES

1. Kunc, V., et al., "Large Scale Additively Manufactured Tooling for Composites." *15th Japan International SAMPE Symposium and Exhibition*. Tokyo, Japan, November 27-December 1, 2017. Society for the Advancement of Material Process Engineering.
2. Hassen, A.A., et al. "Additive Manufacturing of Composite Tooling Using High Temperature Thermoplastic Materials." *SAMPE 2016*, Long Beach, CA, May 23-26, 2016. Society for the Advancement of Material and Process Engineering.
3. Hassen, A.A., et al. "The Durability of Large-Scale Additive Manufacturing Composite Molds." *CAMX 2016*, Anaheim, Ca, September 26-29, 2016. Composites and Advanced Materials Expo.
4. Duty, C.E., et al., "Structure and mechanical behavior of Big Area Additive Manufacturing (BAAM) materials." *Rapid Prototyping Journal* 23 (2017): 181-189. https://doi.org/10.1108/RPJ-12-2015-0183
5. Compton, B.G., et al., "Thermal analysis of additive manufacturing of large-scale thermoplastic polymer composites." *Additive Manufacturing* 17 (2017): 77-86.
6. Hmeidat, N.S., J.W. Kemp, and B.G. Compton, "High-strength epoxy nanocomposites for 3D printing." *Composites Science and Technology* 160 (2018): 9-20. https://doi.org/10.1016/j.compscitech.2018.03.008
7. Compton, B.G. and J.A. Lewis, "3D-Printing of Lightweight Cellular Composites." *Advanced Materials* 26 (2014): 5930-5935. https://doi.org/10.1002/adma.201401804
8. Lewis, J.A., "Direct Ink Writing of 3D Functional Materials." *Advanced Functional Materials* 16 (2006): 2193-2204. https://doi.org/10.1002/adfm.200600434
9. Kunc, V., et al. "Low Cost Reactive Polymers for Large Scale Additive Manufacturing." *CAMX 2018*, Dallas, TX, October 15-18, 2018. Composites and Advanced Materials Expo.
10. Lindahl, J.M., et al. "Large-Scale Additive Manufacturing with Reactive Polymers." *CAMX 2018*, Dallas, TX, October 15-18, 2018. Composites and Advanced Materials Expo.
11. Rios, O., et al., "3D printing via ambient reactive extrusion." *Materials Today Communications* 15 (2018): 333-336.